

Comparative analysis of two types of Cable-suspended Parallel Robots, RSCPR system and RFCPR system

Mirjana Filipovic

Mihajlo Pupin Institute, University of Belgrade
Belgrade, Serbia

e-mail: mira@robot.imp.bg.ac.rs

mirjana.filipovic@pupin.rs

Abstract—Two new CPR structures are proposed in this paper. First structure is Rigid ropes S-type Cable-suspended Parallel Robot, RSCPR system and second structure is Rigid ropes F-type Cable-suspended Parallel Robot, RFCPR system. The high authentic form or general form of CPR mathematical model is defined for two constructions of CPR systems. The kinematic model is defined for each monitored system via the Jacobian matrix. An adequate choice of the generalized coordinates (in this paper, the internal coordinates) provides a dynamic model that illuminates over the Jacobian matrix the mapping of internal (resultant forces of motors) and external forces (acting on a camera carrier) on motion dynamics of each motor. For the calculation of the dynamic model, the Lagrange principle of virtual work has been adopted for RFCPR system because it has two ropes in one direction.

Keywords- cable-suspended parallel robot; abstraction of real systems to models; observantion; workspace; kinematic; dynamic.

Nomenclature

DOF	degree of freedom
CPR	Cable-suspended Parallel Robot
RSCPR	Rigid ropes S-type Cable-suspended Parallel Robot
RFCPR	Rigid ropes F-type Cable-suspended Parallel Robot
$t(s)$	time
$dt = 0.0001(s)$	sample time
$g = 9.81(m/s^2)$	gravitational acceleration
$p = [x \ y \ z]^T$	position of camera carrier in Cartesian space
$i = 1, 2, 3$	total number of DOF
$\theta_i (rad)$	motor shaft angular position after gear box
$\phi = [\theta_1 \ \theta_2 \ \theta_3]^T$	vector of internal coordinates
$F_S = [F_1 \ F_2 \ F_3]^T$	resultant force -RSCPR system
$F_F = [F_1 \ F_2 \ F_3]^T$	resultant force -RFCPR system

$F = [F_x \ F_y \ F_z]^T$	acting force on the camera carrier
$M_S = [M_1 \ M_2 \ M_3]^T$	resultant motor load moment - RSCPR system
$M_F = [M_1 \ M_2 \ M_3]^T$	resultant motor load moment - RFCPR system
$R_1 = 0.06(m) \ R_2 = 0.07(m)$	winch radius
$R_3 = 0.08(m)$	
$J_S (1/m)$	Jacobian matrix -RSCPR system
$J_F (1/m)$	Jacobian matrix -RFCPR system
$O_S (m)$	moment mapping matrix - RSCPR
$O_F (m)$	moment mapping matrix - RFCPR system
$R_{ri} = 0.917(\Omega)$	rotor circuit resistance
$u_i (V)$	voltage
$i_i (A)$	rotor current
$C_{Ei} = 3.3942(V/(rad/s))$	back electromotive force constant
$C_{Mi} = 2.5194(Nm/A)$	constant of the moment proportionality
$B_{Ci} = 0.0670(Nm/(rad/s))$	coefficient of viscous friction
$J_{ri} = 1.5859(kgm^2)$	moment of inertia for the rotor and the gear box
$G_{vi} = \frac{J_{ri} \cdot R_{ri}}{C_{Mi}} = 0.1787$	motor inertia characteristic
$L_{vi} = \frac{R_{ri} \cdot B_{Ci}}{C_{Mi}} + C_{Ei} = 3.4186$	motor damping characteristic
$S_{vi} = \frac{R_{ri}}{C_{Mi}} = 0.364$	motor geometric characteristic
$m = 1(kg)$	mass of the camera carrier

$d = 3.2(m)$	length of the recorded field
$s = 2.2(m)$	width of the recorded field
$v = 2.0(m)$	height of the recorded field
$\delta\theta_i(0)=0(rad), \delta\dot{\theta}_i(0)=0(rad/s)$	initial deviation of the motor angular position
$K_{lpi} = 4200$	positional amplification for motion control
$K_{lvi} = 130$	velocity amplification for motion control
$\diamond = 0.5$	factor that characterize two parallel guided ropes

I. INTRODUCTION

The system for the 3D workspace observation with moving objects has been developed and analyzed worldwide in various research areas for different purposes and with some limitations. The similar research has been done and published.

In paper [1], the design of a planar three-degree-of-freedom parallel manipulator is considered from a kinematic viewpoint. The paper [2] presents the first and second order kinematic analysis of a three-degree-of-freedom 3-RPS parallel robot mechanism. In paper [3] authors present algorithms that enable precise trajectory control of NIMS3D, an under constrained, three-dimensional cabled robot intended for use in actuated sensing. In paper [4] author presents several prototypes of wire-driven parallel robots, recently designed and which use two different actuation schemes. The wrench-closure workspace of parallel cable-driven mechanisms is the set poses of their mobile platform for which the cables can balance any external wrench in [5]. Parallel cable-driven Stewart-Gough platforms consist of an end-effector which is connected to the machine frame by motor driven cables in [6]. The paper [7] presents the recent results from a newly designed parallel wire robot which is currently under construction. Firstly, an overview of the system architecture is given and technically relevant requirements for the realization are identified. The paper [8] presents an auto-calibration method for over constrained cable-driven parallel robots using internal position sensors located in the motors. Wire-driven parallel robot has attracted the interest of researchers since the very beginning of the study of parallel robots [9].

The camera moves quietly and continuously following the observed object. Camera's carrier moves in space freely allowing the capture of objects from above. It gives a unique feeling to the event viewer to follow smoothly from an unusual proximity, and that is very close to the action regardless of the size of observed space. Free motion in space opens up completely new and unique perspective. Implementation of this system uses the latest technical knowledge. A workspace is an area where the camera can move. Motions of the ropes that carry the camera are controlled. Ropes are unwound (or wound), thus reaching any camera position in space. The control system has the operating software, which as a result provides three-dimensional motion of the camera. The commands for the synchronized motion of each winch are

provided, with control of motion of each motor, which ultimately provides three-dimensional continuous camera motion. The carrier that carries the camera does not have a role only of mechanical motion, because through it remote lens (focus, zoom and clarity) is controlled. The gyro sensor, which is installed in the carrier, is stabilized towards the horizon.

The purpose of this paper is to point out the justification and necessity to define a mathematical model of CPR according to the original scientific principles. This paper proposes the application of theoretical methods in solving specific problems rather than the implementation of systems engineering approaches. It is assumed that ropes are rigid.

Future research intend at implementing the elastic ropes (type of nonlinear dynamic elasticity as defined in [10]-[11]) in the mathematical model of the CPR. In this research several different models were developed and new models will be developing for different applications. All these models will be unified according to their similarities into one reconfigurable model, using the approached presented in [12] and [13].

Procedure of defining the dynamic model of the RSCPR system and RSCPR system is presented in Section II. Comparative analysis of simulation results is made in Section III. Section IV gives conclusion.

II. MATHEMATICAL MODEL OF THE RSCPR SYSTEM AND RFCPR SYSTEM

In this paper, two new original CPR systems are synthesized. One of them is marked as RSCPR (see Fig. 1) and second is marked as RFCPR (see Fig. 2). Over the pulley system, ropes are run on the winches (reel) 1, 2, 3, powered by motors. Ropes wind on winches with radius R or they unwind from them. The angular positions of each motor $\theta_1, \theta_2, \theta_3$, winches rotate directly and thus ropes coil or uncoil synchronously and camera carrier moves in the Cartesian space x, y, z . The desired motion trajectory of the camera is defined in x, y, z , Cartesian coordinates, and it is realized by motion of three motors $\theta_1, \theta_2, \theta_3$. To define a dynamic model of the CPR system for observation of moving objects in workspace depicted in Fig.1, it is first necessary to define the external velocity of change of the coordinates $\dot{p} = [\dot{x} \ \dot{y} \ \dot{z}]^T$ and the velocity of change of the internal coordinates $\dot{\phi} = [\dot{\theta}_1 \ \dot{\theta}_2 \ \dot{\theta}_3]^T$. The Jacobian matrix J_S for RSCPR system, see and J_F for RFCPR system maps the velocity vector of the external coordinates \dot{p} into the velocity vector of the internal coordinates $\dot{\phi}$. See [14], [15].

$$\dot{\phi} = J_S \cdot \dot{p}, J_S = \begin{bmatrix} J_{S11} & J_{S12} & J_{S13} \\ J_{S21} & J_{S22} & J_{S23} \\ J_{S31} & J_{S32} & J_{S33} \end{bmatrix} \quad (1)$$

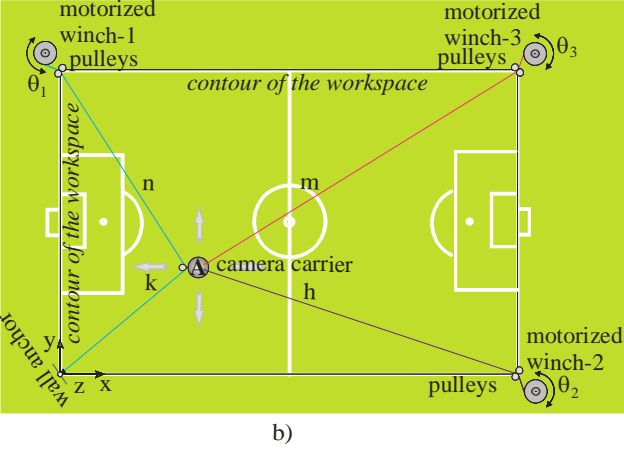
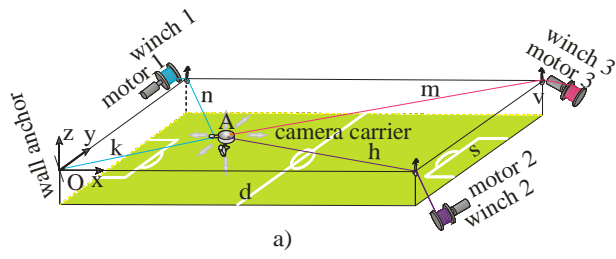


Figure 1. RSCPR system, a) in the 3D space, b) top view

$$\dot{\phi} = J_F \cdot \dot{p}, \quad J_F = \begin{bmatrix} J_{F11} & J_{F12} & J_{F13} \\ J_{F21} & J_{F22} & J_{F23} \\ J_{F31} & J_{F32} & J_{F33} \end{bmatrix} \quad (2)$$

This procedure is named KinRSCPR-Solver or KinRFCPR-Solver (Kinematic Rigid S-type (or F-type) Cable-suspended Parallel Robot Solver). The elements of these J_S and J_F matrices that are beyond the diagonal show the strong coupling between the external and internal coordinates. The mathematical model of the RSCPR and RFCPR system has the form of equation (3) and (4), respectively:

$$u = G_v \cdot \ddot{\phi} + L_v \cdot \dot{\phi} + S_v \cdot M_S \quad (3)$$

$$u = G_v \cdot \ddot{\phi} + L_v \cdot \dot{\phi} + S_v \cdot M_F \quad (4)$$

Where: $u = [u_1 \ u_2 \ u_3]^T$, $G_v = \text{diag } G_{vi}$, $L_v = \text{diag } L_{vi}$, $S_v = \text{diag } S_{vi}$.

Vector equations (3) and (4) are given by applying Lagrange's equation on the generalized coordinates θ_1 , θ_2 , θ_3 . The Lagrange principle of virtual work has been used to find the relation between the resultant moment and external force for RSCPR and RFCPR system has the form of equation (5) and (6), respectively:

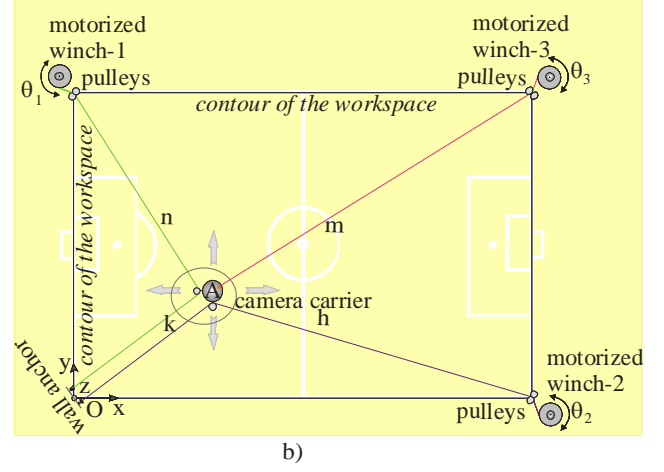
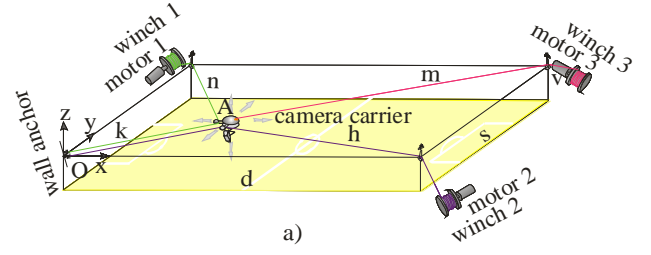


Figure 2. RFCPR system, a) in the 3D space, b) top view

$$M_S = ((J_S)^T)^{-1} \cdot F \quad (5)$$

$$M_F = ((J_F)^T)^{-1} \cdot F \quad (6)$$

The equation (5) can be directly applied to the RSCPR system presented in the Fig. 1, because the RSCPR system has one rope in k , h , m , n directions. See Fig. 3.

The equation (6) cannot be directly applied to the RFCPR system presented in the Fig. 2, because the RFCPR system has two ropes in k direction.

This situation causes the Jacobian matrix J_F in equation (6) to be corrected using the factor \diamond .

\diamond is a factor which multiplies only the direction where there are two parallel ropes. In the k direction, a force in each rope is multiplied by \diamond , which is a half of the whole force F_k . See Fig. 4.

Observed RFCPR system has two ropes from a camera carrier to the wall anchors (line k), and one rope from the camera carrier to the remaining three-point suspension (line h , m , n).

The elements of the matrix J_F which contain the length k are multiplied by a factor \diamond .

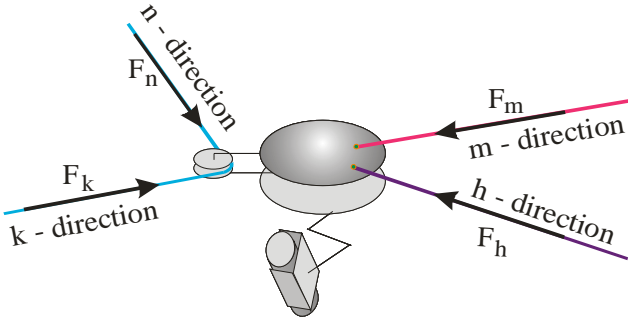


Figure 3. The forces in the RSCPR system camera carrier ropes

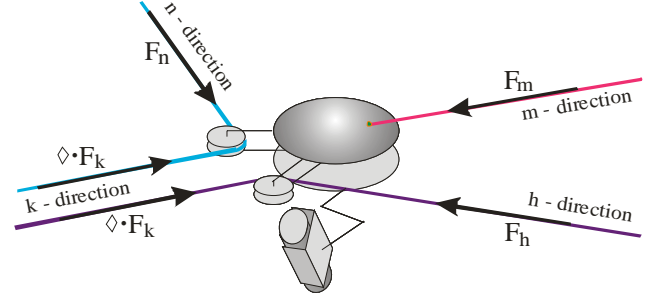


Figure 4. The forces in the RFCPR system camera carrier ropes

Some elements of the Jacobian matrix J_F have the following values $J_{F11} = \frac{x}{R_1 \cdot k} + \frac{x}{R_1 \cdot n}$, $J_{F12} = \frac{y}{R_1 \cdot k} - \frac{(s-y)}{R_1 \cdot n}$, and $J_{F13} = \frac{z}{R_1 \cdot k} + \frac{z}{R_1 \cdot n}$. The elements of the adopted Jacobian matrix $J_{\diamond F}$ have values $J_{\diamond F11} = \diamond \cdot \frac{x}{R_1 \cdot k} + \frac{x}{R_1 \cdot n}$, $J_{\diamond F12} = \diamond \cdot \frac{y}{R_1 \cdot k} - \frac{(s-y)}{R_1 \cdot n}$, and $J_{\diamond F13} = \diamond \cdot \frac{z}{R_1 \cdot k} + \frac{z}{R_1 \cdot n}$, respectively. The adapted Lagrange principle of virtual work defined in equation (7) has been used for solving the complex relation between the resultant moment M_F and external force F .

$$M_F = \left((J_{\diamond F})^T \right)^{-1} \cdot F \quad (7)$$

The moment mapping matrix for RSCPR and RFCPR system is defined in equation. (8) and (9), respectively:

$$O_S = \left((J_S)^T \right)^{-1} \quad (8)$$

$$O_F = \left((J_{\diamond F})^T \right)^{-1} \quad (9)$$

The equation (10) and (11) are obtained by substituting (5) into the (3) and (7) into the (4), respectively:

$$u = G_v \cdot \ddot{\phi} + L_v \cdot \dot{\phi} + S_v \cdot O_S \cdot F \quad (10)$$

$$u = G_v \cdot \ddot{\phi} + L_v \cdot \dot{\phi} + S_v \cdot O_F \cdot F \quad (11)$$

The moment mapping matrix O_S (O_F) characterizes a strong coupling between the presented motors. Control law is selected by the local feedback loop for position and velocity of the motor shaft in the following form:

$$u_i = K_{pi} \cdot (\theta_i^o - \theta_i) + K_{vi} \cdot (\dot{\theta}_i^o - \dot{\theta}_i) \quad (12)$$

III. SIMULATION RESULTS

In order to make the results comparable, the simulation results are made for the same desired trajectory and the same all other system parameters, as defined in the Nomenclature. The camera moves in the 3D space in x , y , and z directions. The camera carrier has the starting point $p_{start}^o = [2.3 \ 1.8 \ -0.3](m)$, and the end point $p_{end}^o = [1.6 \ 0.4 \ -0.8](m)$. The camera moves in x , y , and z directions and its velocity has a trapezoidal form with maximum velocity $\dot{p}_{max}^o = 0.417(m/s)$. The selected motors are by Heinzman SL100F and selected gear boxes are HFUC14-50-2A-GR+belt. The RSCPR mathematical model at the reference and real frame is defined by the equations (1), (3), (5), (8) and (10). The RFCPR mathematical model at the reference and real frame is defined by the equations (2), (4), (7), (9) and (11). The dynamic responses, for both systems are shown in Fig. 5 and 6. Each example has six pictures related to the:

- camera carrier position at the reference and the real frames,
- motor shaft position at the reference and the real frames,
- forces in the ropes at the reference and the real frames,
- deviation between the real and the reference trajectory of the camera carrier,
- deviation between the real and the reference trajectory of the motor shaft positions,
- reference and the real control signals.

The RSCPR system shows a good response. See Fig. 5, unlike the RFCPR system. See Fig. 6. The tracking of the motors angular positions θ_2 will be bad in periods when the motor 2 is in saturation. This indirectly causes poor tracking of the desired trajectory in the Cartesian space for x , y , and z directions.

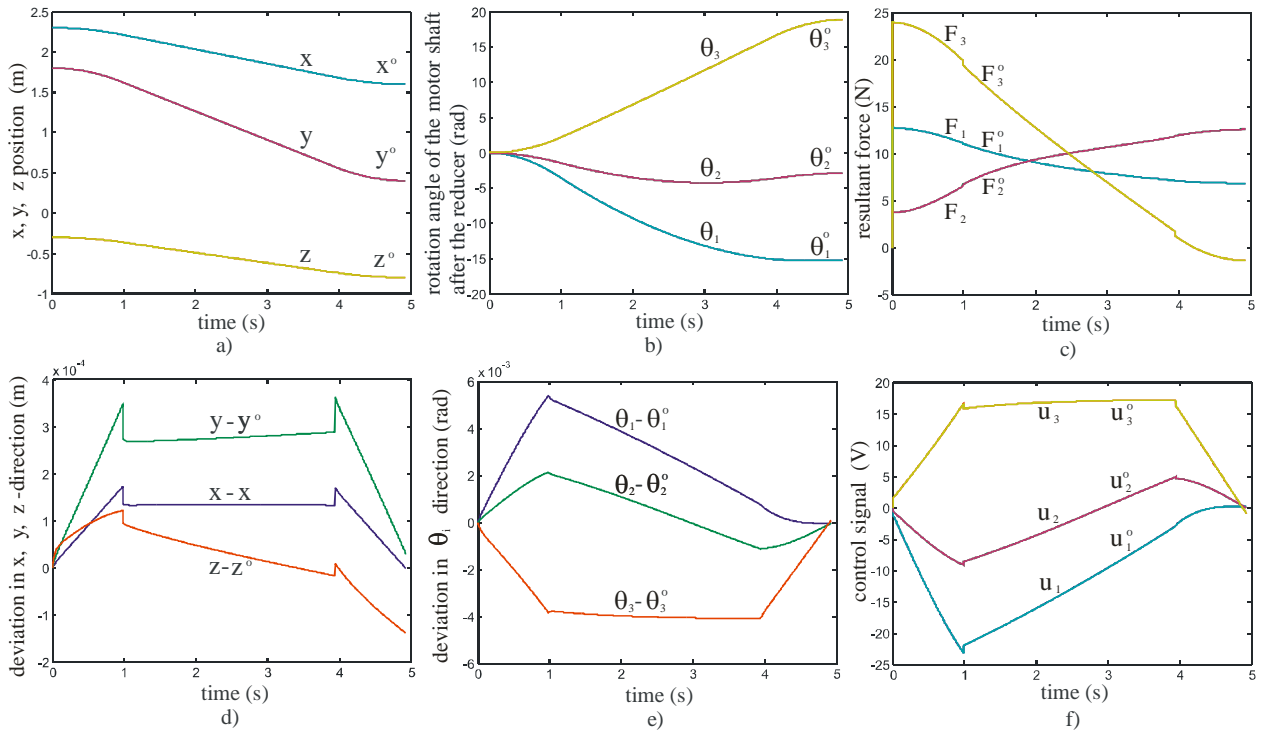


Figure 5. Simulation results for RSCPR system

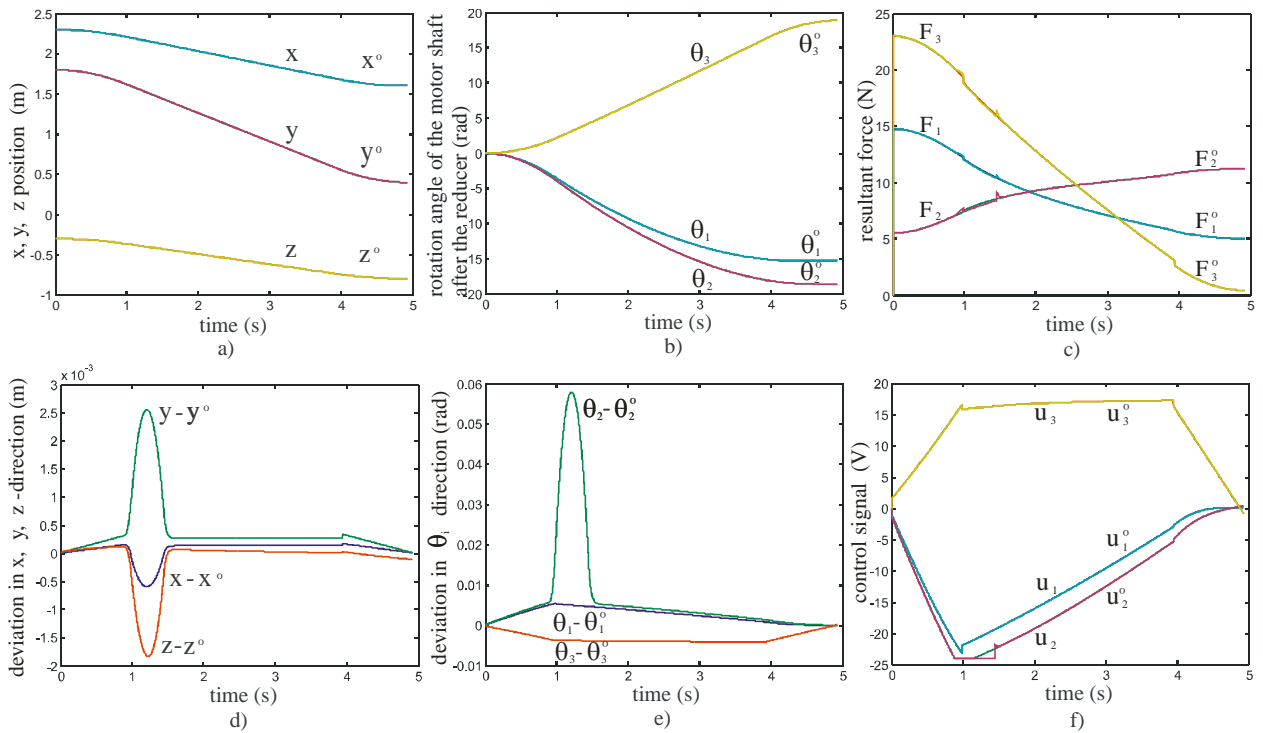


Figure 6. Simulation results for RFCPR system

TABLE I. COMPARISON OF TWO CPR CONFIGURATIONS

	<i>RSCPR system</i>	<i>RFCPR system</i>
Fig.	5	6
motors saturation	no	yes

RSCPR system is modeled and analyzed by software package ORIGI but RFCPR system is modeled and analyzed by software package ORVER. The software packages ORIGI and ORVER provide the ability for a comparative analysis of these systems from different aspects. This analysis shows that the motion dynamics of individual CPR depends significantly on the CPR's construction type and its parameters as well.

IV. CONCLUSION

High authentic form or general form mathematical model is defined for two constructions of RSCPR and RFCPR. Kinematic model is defined for each monitored system via the Jacobian matrix. This methodology for developing the kinematic model of selected CPR systems is named the KinRSCPR-Solver or KinRFCPR-Solver (Kinematic Rigid S-type (or F-type) Cable-suspended Parallel Robot Solver), and it gives a precise direct and inverse kinematic solutions. An adequate choice of generalized coordinates provides a dynamic model that illuminates the mapping of internal (resultant forces of motors) and external forces (acting on a camera carrier) over the Jacobian matrix on motion dynamics of each motor. For the computation of the dynamic model, the Lagrange principle of virtual work is applied (and adopted for RFCPR system). Software packages ORIGI and ORVER are formed and used for individual and comparative analysis of CPR from various aspects. The goal is comparison of these two constructions, RSCPR and RFCPR, for the same parameters (workspace dimensions, the mass of a camera carrier, change the size and dynamics of power disturbances, the choice of control law, the reference trajectory, and the presence of singularity avoidance system and a number of other characteristics). The choice of the type of construction of CPR is especially emphasized. The simulation results present how a chosen construction of CPR type affects the motors load, control signals, etc. The construction type can significantly influence the response of the system or accuracy of tracking the desired trajectory.

The aim of this study is to define the characteristics of CPR and all this for the purpose of modernization and wider application of the same.

ACKNOWLEDGMENT

This research has been supported by the Ministry of Education, Science and Technological Development, Government of the Republic of Serbia Grant TR-35003 through the following two projects: "Ambientally intelligent service robots of anthropomorphic characteristics," by Mihajlo Pupin Institute, University of Belgrade, Serbia, Grant OI-174001 and "The dynamics of hybrid systems of complex structure," by Institute SANU Belgrade and Faculty of

Mechanical Engineering University of Nis, Serbia, and partially supported by the project SNSF Care-robotics project no. IZ74Z0-137361/1 by Ecole Polytechnique Federale de Lausanne, Switzerland.

We are grateful to Prof. Dr. Katica R. (Stevanovic) Hedrih from Mathematical Institute, Belgrade for helpful consultations during the implementation of this paper.

REFERENCES

- [1] C. Gosselin, and J. Angeles, "The Optimum Kinematic Design of a Planar Three-Degree-of-Freedom Parallel Manipulator," *Journal of Mechanisms, Transmissions, and Automation in Design*, Vol. 110/35-41, March 1988.
- [2] J. Fang, and Z. Huang, "Kinematics of a three-degree-of-freedom in-parallel actuated manipulator mechanism," *Mech. Mach. Theory*, Vol. 32, No 7, pp. 789-796, 1997.
- [3] P.H. Borgstrom, N.P. Borgstrom, M. J. Stealey, B. Jordan, G. Sukhatme, M. A. Batalin, and W. J. Kaiser, "Discrete Trajectory Control Algorithms for NIMS3D, an Autonomous Underconstrained Three-Dimensional Cabled Robot," *Proceedings of the 2007 IEEE/RSJ International Conference on Intelligent Robots and Systems*, San Diego, CA, USA, Oct 29 - Nov 2, 2007.
- [4] J.P. Merlet, MARIONET, "A Family of Modular Wire-Driven Parallel Robots," *Advances in Robot Kinematics: Motion in Man and Machine*, Part 1, pp. 53-61, 2010.
- [5] M. Gouttefarde, J.-P. Merlet, and D. Daney, "Determination of the wrench-closure workspace of 6-DOF parallel cable-driven mechanisms," *Advances in Robot Kinematics*, Part 5, 315-322, 2006.
- [6] T. Bruckmann, L. Mikelsons, D. Schramm, and M. Hiller, "Continuous workspace analysis for parallel cable-driven Stewart-Gough platforms," *Special Issue: Sixth International Congress on Industrial Applied Mathematics (ICIAM07) and GAMM Annual Meeting, Zürich 2007*, Volume 7, Issue 1, December 2007.
- [7] A. Pott, "Forward Kinematics and Workspace Determination of a Wire Robot for Industrial Applications," *Advances in Robot Kinematics: Analysis and Design*, Part 7, pp. 451-458, 2008.
- [8] P. Miermeister, A. Pott, and A. Verl, "Auto-Calibration Method for Overconstrained Cable-Driven Parallel Robots," *ROBOTIK 2012 - 7th German Conference on Robotics*, Munich, Germany, 2012.
- [9] T. Higuchi, A. Ming, and J. Jiang-Yu, "Application of multi-dimensional wire crane in construction," *In 5th Int. Symp. on Robotics in Construction*, pp. 661-668, Tokyo, June, 6-8, 1988.
- [10] K. (Stevanovic) Hedrih, "Transversal forced vibrations of an axially moving sandwich belt system," *ARCH APPL MECH*, Springer, 78(9), pp. 725-735, 2008.
- [11] K. (Stevanovic) Hedrih, "Vibration Modes of a axially moving double belt system with creep layer," *J VIB CONTROL*, 14(10-Sep), pp. 1333-1347, 2008.
- [12] A. Djuric, R. Al Saidi, and W.ElMaraghy, "Dynamics Solution of n-DOF Global Machinery Model," *Robotics and Computer Integrated Manufacturing (CIM) Journal*, 28(5) 621-630, 2012.
- [13] A. M. Djuric, R. Al Saidi, and W. H. ElMaraghy, "Global Kinematic Model Generation for n-DOF Reconfigurable Machinery Structure," *6th IEEE Conference on Automation Science and Engineering*, CASE 2010, Toronto, Canada, (2010), August 21-24, 2010.
- [14] R P. Paul, *Robot Manipulators: Mathematics, ming, and Control*, The Computer Control of Robot Manipulators," The MIT Press, Cambridge, Massachusetts and London, England, 1981.
- [15] J. Denavit, and R S. Hartenberg, "A Kinematic Notation for Lower-pair Mechanisms Based on Matrices," *Journal of Applied Mechanics*, Vol. 77, pp. 215-221, 1955.